A Bidirectional Multilevel DC-DC Converter Applied to a Bipolar DC Grid: Analysis of Operation under Fault Conditions

Cátia F. Oliveira
Centro ALGORITMI
University of Minho
Guimarães, Portugal
c.oliveira@dei.uminho.pt

João L. Afonso
Centro ALGORITMI
University of Minho
Guimarães, Portugal
jla@dei.uminho.pt

Vítor Monteiro
Centro ALGORITMI
University of Minho
Guimarães, Portugal
vmonteiro@dei.uminho.pt

Abstract—**Recently, DC grids have been an important subject of research due to their attractive features comparing with AC grids. The characteristic advantages of DC grids are not only related with the integration of native DC technologies, as renewable energy sources (RES) and energy storage systems (ESS), but also with the reduced number of power converters. Relatively to the configurations of DC grids, in this paper, it is presented a bipolar DC grid, where an innovative bidirectional multilevel DC-DC converter is considered under a fault-tolerance analysis. This converter can be used to interface with several technologies, but, in the scope of this paper, it is considered the application of an electric vehicle (EV) battery charger. Taking into account that some failures can occur, namely in the DC-DC converter and in the bipolar DC grid, the operation of the DC-DC converter within the bipolar DC grid can be harmful. Therefore, this paper also presents a fault-tolerance analysis of the DC-DC converter when facing the occurrence of failures in itself and in the bipolar DC grid, namely for different scenarios of failure in the DC-link wires. Besides, the control strategy for the DC-DC converter is described in detail for distinct scenarios of operation, both in steady-state and transient-state.**

Keywords—Bipolar DC Grids, EV Battery Charger, Fault-Tolerance, Multilevel DC-DC Converter.

I. INTRODUCTION

The increasing power consumption, the use of fossil fuels as the primary energy source in the world, and the low power quality represents a huge concern that requires special attention in order to improve the power grid as a whole [1][2]. DC grids can be part of an innovative solution to tackle these problems. The reduction of power losses and the power flow improvement become DC grids an attractive solution for distributed generation (DG) units [3]. DC grids have the particularity of being very beneficial to DG due to the efficiency of power exchange and the integration of native DC technologies, as energy storage systems (ESS) and renewable energy sources (RES) [4]. Thus, DC grids contribute to a cleaner environment due to the introduction of RES, namely the PV panels and fuel-cells to generate as much of DC power as possible. On the other hand, the increasing use of DC loads such as electric vehicles (EV), LEDs lighting, and personal computers, become the DC grids fundamental for their operation [5][6]. In DC grids, several technologies, infrastructures and systems can be included, such as: hybrid energy storage systems [7]–[9], smart homes [10]–[12], renewable energy parks [13]–[15], and EV charging stations [16]–[18]. Moreover, DC grids present many advantages comparing to the traditional AC grids, e.g., the efficiency is higher due to the minimization of power losses caused by the power conversion of AC-DC converters [19]. On the other hand, in case of failures in the AC grid, DC grids can be disconnected and continue operating correctly [20], which means that DC grids can operate independently (stand-alone operation) or operate in conjunction with the grid (grid-connected mode) [21].

Over the years, many studies have been conducted in different DC grids configurations and control strategies [22]-[26]. Relatively to DC grids configurations, there are two main structures: the unipolar and the bipolar. Both configurations present advantages and disadvantages. The unipolar configuration is simpler in terms of control and it is less complex since it has only two wires, which means that carry only one DC voltage level. However, the case of bipolar DC grids is quite different because this configuration is composed by three wires, so the complexity of the control is evident comparing with the unipolar configuration. Despite that, the bipolar DC grids present two DC voltage levels and due to the number of wires that compose this type of structure, the bipolar DC grids allow the integration of power converters of different voltage levels. Moreover, in case of failure of one wire, the bipolar DC grid can continue operating. However, in case of the interface of power converters of three wires, when the occurrence of failures of only one wire of the bipolar DC grid, it is important that the operation of the power converters is not affected.

In this context, this paper presents a bidirectional multilevel DC-DC converter [27][28] applied as interface of an EV battery charger as illustrated in Fig. 1. The multilevel DC-DC converter is validated for different cases, namely the presence of failures in the positive wire, negative wire, or the neutral wire of the bipolar DC grid. The validation of the DC-DC converter is carried out without any additional hardware to prove the fault-tolerance of the power converter.
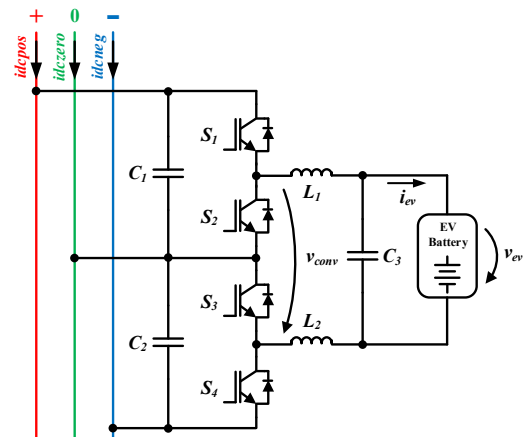

Fig. 1. Multilevel DC-DC converter under analysis, connected to a bipolar DC grid, and applied as interface of an EV battery charger.

II. Operating Principle of the Multilevel DC-DC Converter

In this section is described in detail the operating principle of the presented multilevel DC-DC converter in two different scenarios, namely under normal conditions and under fault conditions. Under normal conditions, it is not verified any fault in bipolar DC grid, whereas under fault conditions the operation of the multilevel DC-DC converter is analyzed in three different faults that can occur in bipolar DC grid, such as failures in the positive wire, neutral wire and negative wire.

A. Normal Conditions

The bidirectional DC-DC converter is perfectly suitable for a bipolar DC grid due to the middle point which allows the connection of the power converter to three wires of the DC grid. Moreover, the multilevel DC-DC converter is a good solution to interface an EV battery charger, presenting two operation modes: buck-mode to charge the EV battery and boost-mode to discharge the EV battery to the grid. In this paper, it is analyzed the buck-mode operation for the EV battery charging. The bidirectional DC-DC converter is composed by four semiconductors totally controlled, in this case IGBTs, and a split DC-link. Moreover, connected to the power converter there is a LC passive filter in the interface of the EV. Depending on the states of the four IGBTs, the bidirectional DC-DC converter produces three different voltage levels, 0, $+v_{dc}/2$ and $+v_{dc}$. During the EV battery charging process, which corresponds to the buck-mode operation, when the S_1 and S_4 are enabled the EV battery and the inductors L_1 and L_2 are charged from the capacitors C_1 and C_2 which composes the DC-link. The output DC voltage of the DC-DC converter is $+v_{dc}$. When the IGBTs S_1 and S_4 are disabled, the EV battery is charged through the energy stored by the inductors L_1 and L_2 and the output voltage of the DC-DC converter is 0 V. In case of only one IGBT S_1 or S_4 is enabled, the EV battery and the inductors L_1 and L_2 store energy from the split DC-link, whose output voltage produced by the DC-DC converter is $+v_{dc}/2$. As mentioned above, in this paper the DC-DC converter operation is only analyzed for the buck-mode, so the semiconductors S_2 and S_3 never switch.

B. Fault Conditions

The aim of this paper is to analyze the performance of the multilevel DC-DC converter under different fault conditions. Fig. 2 presents the operation modes of the DC-DC converter under a failure in the positive wire of the DC grid. As it can be observed, the EV battery can be charged in only two forms: (a) When the current flows through the antiparallel diode of the IGBT S_2 and the IGBT S_4; (b) When the current flows through the antiparallel diodes of the IGBTs S_2 and S_3. Both operation modes are applied when the EV battery current, i_{ev} is higher or lower than the reference current. On the other hand, the failures in bipolar DC grid can occur in the neutral and negative wires. Fig. 3 and Fig. 4 demonstrate both failures occurrences, respectively. In case of occurrence of a failure in neutral wire of the DC grid, the current flows through the IGBTs S_1 and S_4 (Fig. 3(a)) or through the antiparallel diodes of the IGBTs S_2 and S_3 (Fig. 3(b)). In the presence of a failure in the negative wire of the DC grid, the EV battery is charging when the current flows through the IGBTs S_1 and the antiparallel diode of the IGBT S_3 (Fig. 4(a)) or when the current flows through the antiparallel diodes of the IGBTs S_2 and S_3 (Fig. 4(b)), depending on the i_{ev} in relation to the established reference current.
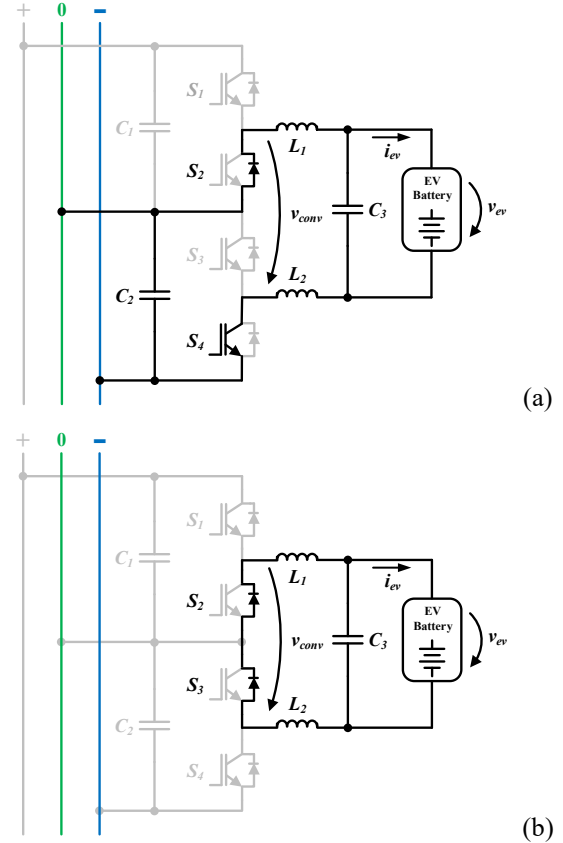

(a)

(b)

Fig. 2. Operation modes of the DC-DC converter under a failure in the positive wire of the bipolar DC grid: (a) When v_{conv} is $+v_{dc}/2$; (b) When v_{conv} is 0.
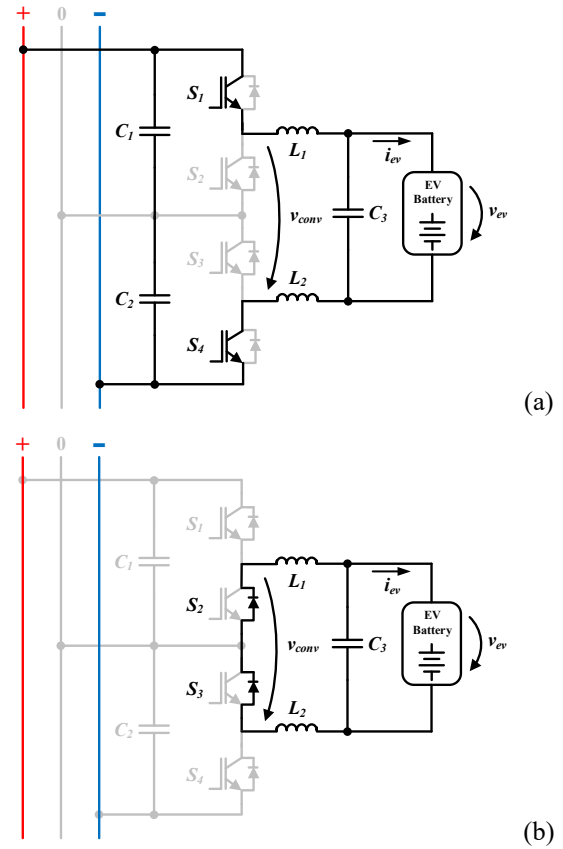

(a)

(b)

Fig. 3. Operation modes of the DC-DC converter under a failure in the neutral wire of the bipolar DC grid: (a) When v_{conv} is $+v_{dc}$; (b) When v_{conv} is 0.
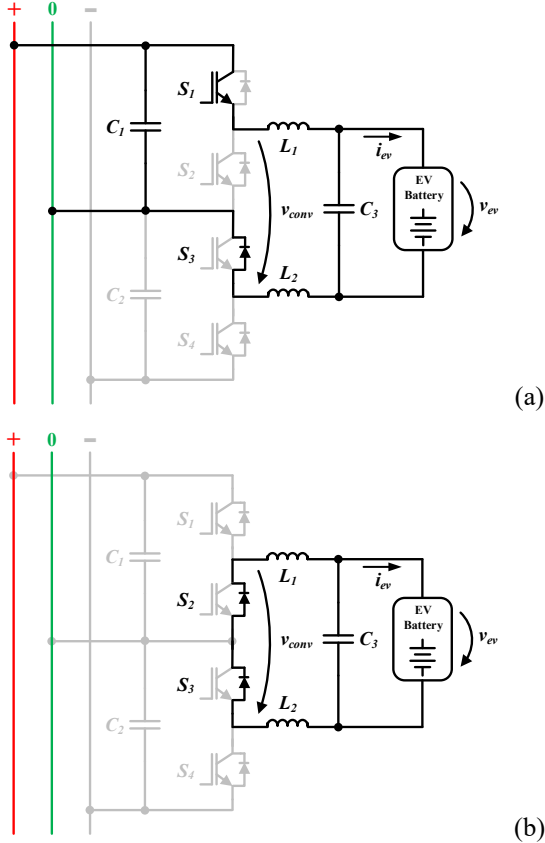
(a)

(b)

Fig. 4. Operation modes of the DC-DC converter under a failure in the negative wire of the bipolar DC grid: (a) When v_{conv} is $+v_{dc}/2$; (b) When v_{conv} is 0.

III. CONTROL OF THE MULTILEVEL DC-DC CONVERTER

In this section is described the control strategy to the EV battery charging for normal conditions or in the presence of failures in the bipolar DC grid. The presented control strategy is also applied during the steady-state operation and during the transient-state operation.

Therefore, the voltage synthetized by the multilevel DC-DC converter is presented as v_{conv}, whose value corresponds to the sum of the EV battery voltage, v_{ev}, with the voltage in the inductor L_1, v_{L1}, and the voltage in the inductor L_2, v_{L2}, as demonstrated in (1):

$$v_{conv} = v_{ev} + v_{L1} + v_{L2} \qquad (1)$$

Knowing that the current in the inductors L_1 and L_2 are equal, thus the equation (1) can be rewritten as presented in (2):

$$v_{conv} = v_{ev} + (L_1 + L_2)\frac{di_{ev}}{dt} \qquad (2)$$

Applying the Euler method, the voltage that the bidirectional multilevel DC-DC converter must be synthetized in the period between k and $k + 1$ is established as demonstrated in (3):

$$v_{conv} = v_{ev} + (L_1 + L_2) f_s \left(i_{ev}[k + 1] - i_{ev}[k] \right) \qquad (3)$$

where f_s corresponds to the sampling frequency, $i_{ev}[k + 1]$ corresponds to the reference current that must be reached and $i_{ev}[k]$ is the EV battery current at the instant k.

The resulting voltage v_{conv} is compared to two triangular carriers 180º phase shifted, whose comparison results in the control signals of the IGBTs S_1 and S_4 in normal conditions.

IV. VALIDATION OF THE MULTILEVEL DC-DC CONVERTER

After a detailed description of the control strategy adopted for the multilevel DC-DC converter, it is validated and analyzed the EV battery charging for steady-state and transient-state operations in two distinct scenarios: normal conditions and failure conditions in bipolar DC grid. The presented results are validated in the simulation software PSIM. For the development of the simulation, it was considered a sampling frequency of 40 kHz and a switching frequency of 20 kHz. Relatively to the passive elements, the L_1 and L_2 value is 1.2 mH. To validate all operation modes was considered for a DC-link voltage for each capacitor (C_1 and C_2) a voltage value of 200 V, whereas the EV battery voltage is 100 V.

A. EV Battery Charging: Steady-State Operation

The EV battery charging during the steady-state operation is presented in Fig. 5, Fig. 6 and Fig. 7. Fig. 5 shows the principle of operation of the bidirectional DC-DC converter for a reference current of 10 A and the output voltage of the converter v_{conv} varies between 0 V and 200 V, whose maximum value corresponds to half of the total voltage in DC-link. Initially, there is not any failure in the bipolar DC grid, however at the time of approximately 0.015 s occurs a failure in the positive wire of the DC grid. As it can be observed, due to this failure the current in the positive wire i_{dcpos} is zero and the semiconductor S_1 stops switching. Moreover, the duty-cycle observed in semiconductors S_3 and S_4 changes from 25 % to 50 %. Despite that, the DC-DC converter continues operating and the EV battery current i_{ev} reaches a reference current of 10 A. This is only possible because the current flows through the antiparallel diode of the IGBT S_2, though the semiconductor S_1 being disabled. However, the ripple frequency of the EV battery current is higher in the presence of the failure since the ripple frequency of i_{ev} presents a lower value (20 kHz) comparing to the observed in normal conditions.
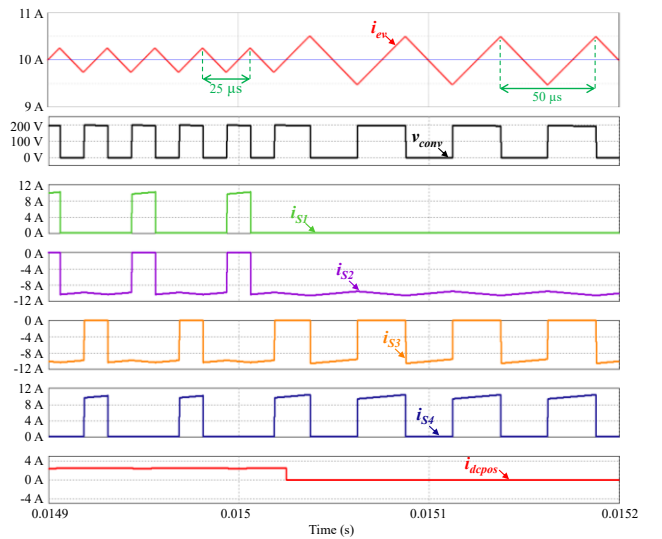

Fig. 5. Steady-state operation of the DC-DC converter under a failure in the positive wire of the bipolar DC grid.

Fig. 6 shows the steady-state operation of the DC-DC converter for a reference current of 8 A. Initially, the converter is operating in normal conditions and the ripple frequency of the i_{ev} is twice the switching frequency (20 kHz). At the instant 0.03 s occurs a failure in the neutral wire of the bipolar DC grid. As it is observed in latter case, the ripple of the i_{ev} is higher than in normal conditions, due to the fact that the ripple frequency of the i_{ev} is equal to the switching frequency. Moreover, the v_{conv} of the DC-DC converter is double of the voltage value verified in normal conditions, which corresponds to the total voltage of the DC-link (400 V). In relation to the semiconductors, depending on the i_{ev} value, the current flows through the semiconductors S_1 and S_4 or S_2 and S_3.
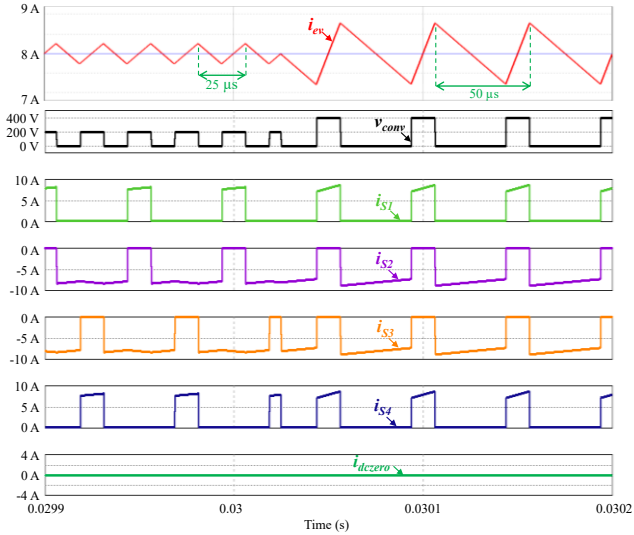

Fig. 6. Steady-state operation of the DC-DC converter under a failure in the neutral wire of the bipolar DC grid.

Fig. 7 illustrates the operation of the DC-DC converter in normal conditions and in the occurrence of a failure in the negative wire of the bipolar DC grid. At the time 0.045 s occurs a failure in the negative wire of the DC grid, where it can be observed that the value of the current in that wire i_{dcneg} is zero. Moreover, the current in the semiconductor S_4, i_{S4} is null and the current starts flowing by the antiparallel diode of
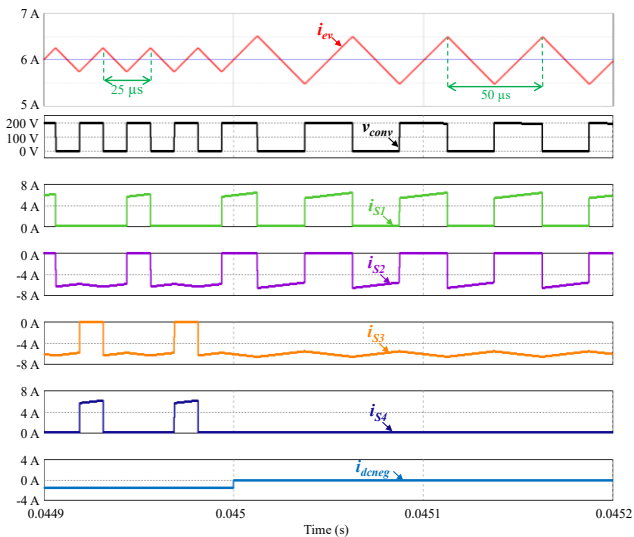

Fig. 7. Steady-state operation of the DC-DC converter under a failure in the negative wire of the bipolar DC grid.

the IGBT S_3 which allows the converter to continue operating and the i_{ev} reaches the established reference current. The duty-cycle of the semiconductors S_1 and S_2 is double (50 %) of the duty-cycle verified in normal conditions (25 %).

In normal conditions, the v_{conv} is compared with two triangular carriers phase shifted 180º, thus the ripple frequency of the i_{ev} is double of the switching frequency (20 kHz), which corresponds of a 40 kHz. However, in the presence of a failure in one of wires of the bipolar DC grid, the ripple frequency of the i_{ev} is the same value of the switching frequency. Due to this fact, the ripple of the current under fault conditions is higher than in normal conditions. Despite that, the DC-DC converter continues operating correctly, observing that the current in the EV battery reaches the established reference current.

B. EV Battery Charging: Transient-State Operation

Fig. 8 illustrates the transient-state operation of the EV battery charger in normal conditions, which means that not occur any type of failure in DC grid. Initially, it was considered a reference current of 12 A and at the time 0.005 s the reference current was reduced to 10 A, whose sudden transition took 50 μs. The figure also demonstrates the current in each semiconductor and v_{conv} whose value varies between 0 V and 200 V. The ripple frequency of the i_{ev} is twice the switching frequency as expected for the normal operation of this converter.
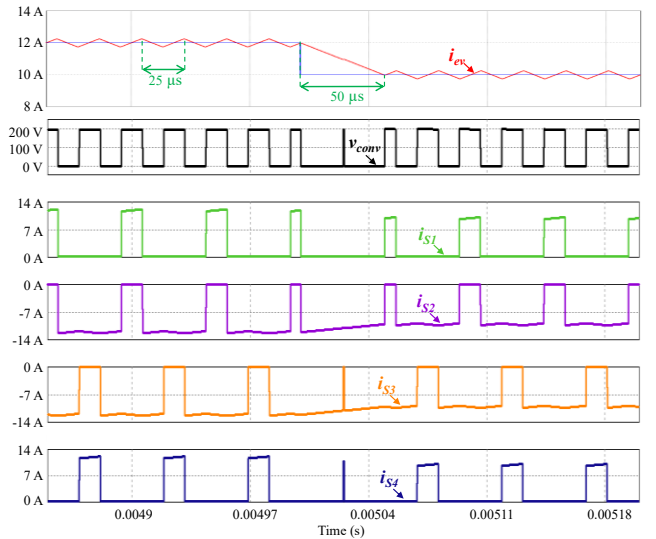

Fig. 8. Transient-state operation of the DC-DC converter in normal conditions of the EV battery charging.

Fig. 9 shows the transient-state operation for the EV battery charging during the occurrence of a failure in the positive wire in the DC grid. As it can be observed the current in the positive wire of the DC grid, i_{dcpos} is zero due to the presence of a failure in this wire. Moreover, the ripple frequency of the i_{ev} is half of the ripple verified in normal conditions, but the transient time of the sudden transition from 10 A to 8 A is the same value (50 μs). Despite the occurrence of a failure, the transition time maintains the same value.

In this situation, the current in semiconductor S_1 is zero and thus the current flows by the semiconductor S_2 as demonstrated in Fig. 2.
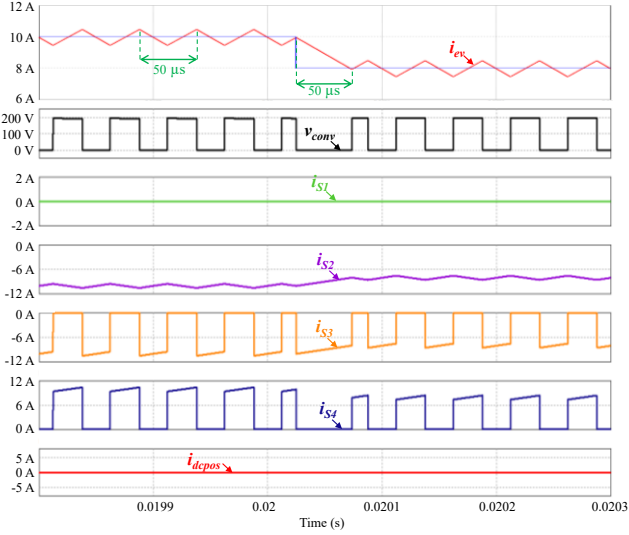
Fig. 9. Transient-state operation of the DC-DC converter under a failure in the positive wire of the bipolar DC grid.

Fig. 10 shows the transient-state operation for the EV battery charging during the occurrence of a failure in the neutral wire of the DC grid. Initially, the reference current is 8 A and at 0.035 s the reference current is changed to 6 A. This sudden transition also takes 50 μs as observed previously, which means that despite the occurrence of a failure, the transition time is not affected. On the other hand, v_{conv} varies between 0 V and 400 V, whose maximum value corresponds to the total voltage of the DC-link. The ripple frequency of the i_{ev} is 20 kHz, which corresponds to the value of the switching frequency. In this figure can also be observed the current in each semiconductor.
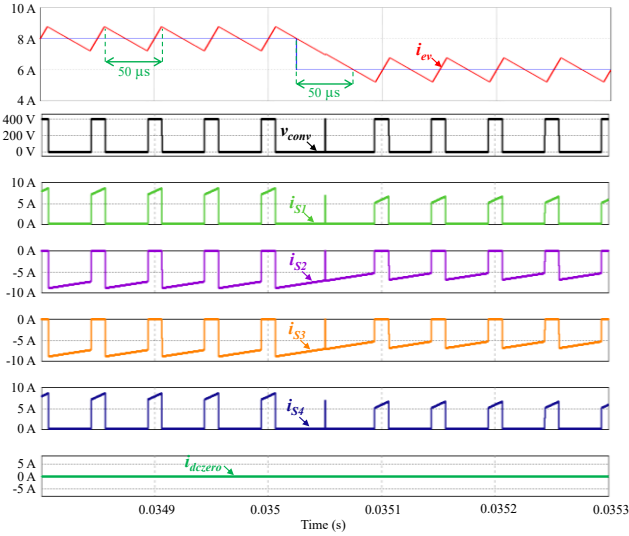

Fig. 10. Transient-state operation of the DC-DC converter under a failure in the neutral wire of the bipolar DC grid.

Finally, Fig. 11 shows the transient-state operation for the EV battery charging during the occurrence of a failure in the negative wire of the DC grid. Initially, it is considered a reference current of 6 A and at the time 0.05 s the reference current is reduced to 4 A. As in previous cases, the transition time is the same (50 μs) and in case of the failures the ripple frequency is 20 kHz, the same value of the switching frequency, which explains that the ripple is higher than is verified in normal conditions. In case of a failure in the negative wire, the current in the semiconductor S_4 is zero and

the current flows by the antiparallel diode of the semiconductor S_3. The v_{conv} varies between 0 V and 200 V.
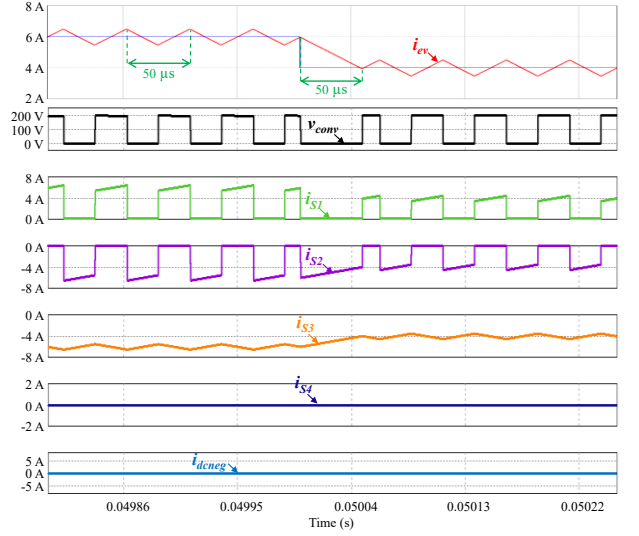

Fig. 11. Transient-state operation of the DC-DC converter under a failure in the negative wire of the bipolar DC grid.

V. CONCLUSIONS

This paper presents a detailed operation analysis of a multilevel DC-DC converter under fault conditions in bipolar DC grids. Besides, the multilevel DC-DC converter is also analyzed in normal conditions. The fault conditions include failures in the positive, neutral and negative wires of the bipolar DC grid. Moreover, the control strategy is described and applied during steady-state and transient-state operations. Throughout the paper, it is demonstrated that the multilevel DC-DC converter operates properly for normal conditions and also in the occurrence of failures. However, the ripple of the current in the electric vehicle (EV) battery under fault conditions is slightly higher than the ripple verified in normal conditions. This occurs because, in the occurrence of failures, the frequency of the ripple of the EV battery current becomes equal to the switching frequency, instead of being twice the switching frequency, as observed in normal conditions. Despite that, in transient-state operation the sudden transitions for different reference currents take the same time in normal conditions and in fault conditions. Moreover, the EV battery current in the presence of a failure in the DC grid is kept constant, and perfectly follows the established reference current. Thus, it can be concluded that the presented DC-DC converter has a good performance, both under normal or fault conditions, ensuring the correct charging of the EV battery.

REFERENCES

[1] E. Unamuno and J. A. Barrena, "Hybrid ac/dc microgrids - Part I: Review and classification of topologies," *Renewable and Sustainable Energy Reviews*, vol. 52, pp. 1251–1259, 2015.

[2] N. Manoj Kumar, S. S. Chopra, A. A. Chand, R. M. Elavarasan, and G. M. Shafiullah, "Hybrid renewable energy microgrid for a residential community: A techno-economic and environmental perspective in the context of the SDG7," *Sustainability (Switzerland)*, vol. 12, no. 10, pp. 1–30, 2020.

[3] N. W. A. Lidula and A. D. Rajapakse, "Microgrids research: A review of experimental microgrids and test systems," *Renewable and Sustainable Energy Reviews*, vol. 15, no. 1, pp. 186–202, 2011.

[4] T. T. H. Ma, H. Yahoui, H. G. Vu, N. Siauve, and H. Morel, "A control strategy of DC building microgrid connected to the neighborhood and AC power network," *Buildings*, vol. 7, no. 2, 2017.

[5] J. J. Justo, F. Mwasilu, J. Lee, and J. W. Jung, "AC-microgrids versus DC-microgrids with distributed energy resources: A review," *Renewable and Sustainable Energy Reviews*, vol. 24, pp. 387–405, 2013.

[6] J. H. Lee, H. J. Kim, B. M. Han, Y. S. Jeong, H. S. Yang, and H. J. Cha, "DC micro-grid operational analysis with a detailed simulation model for distributed generation," *Journal of Power Electronics*, vol. 11, no. 3, pp. 350–359, 2011.

[7] M. Ahmed, S. Kuriry, M. D. Shafiullah, and M. A. Abido, "DC Microgrid Energy Management with Hybrid Energy Storage Systems," *2019 23rd International Conference on Mechatronics Technology, ICMT 2019*, no. Dc, pp. 1–6, 2019.

[8] F. Zhang *et al.*, "Power management strategy research for DC microgrid with hybrid storage system," *2015 IEEE 1st International Conference on Direct Current Microgrids, ICDCM 2015*, no. Dc, pp. 62–68, 2015.

[9] B. Wang, U. Manandhar, X. Zhang, H. B. Gooi, and A. Ukil, "Deadbeat Control for Hybrid Energy Storage Systems in DC Microgrids," *IEEE Transactions on Sustainable Energy*, vol. 10, no. 4, pp. 1867–1877, 2019.

[10] H. Kakigano *et al.*, "Fundamental characteristics of DC microgrid for residential houses with cogeneration system in each house," *IEEE Transactions on Industrial Electronics*, vol. 61, no. 8, pp. 1–8, 2014.

[11] C. Jin, P. Wang, J. Xiao, Y. Tang, and F. H. Choo, "Implementation of hierarchical control in DC microgrids," *IEEE Transactions on Industrial Electronics*, vol. 61, no. 8, pp. 4032–4042, 2014.

[12] Tomislav Dragicevic, Xiaonan Lu, J. C. Vasquez and M. Josep, "DC Microgrids –Part II: A Review of Power Architectures, Applications and Standardization Issues," *IEEE Transactions on Power Electronics*, vol. 31, no. 5, pp. 3528–3549, 2016.

[13] R. Duarte, L. Moreira, L. A. M. Barros, V. Monteiro, J. L. Afonso, and J. G. Pinto, "Power converters for a small islanded microgrid based on a micro wind turbine and an battery energy storage system," *ECOS 2018 - Proceedings of the 31st International Conference on Efficiency, Cost, Optimization, Simulation and Environmental Impact of Energy Systems*, 2018.

[14] M. H. F. Ahamed, U. D. S. D. Dissanayake, H. M. P. de Silva, H. R. C. G. P. Pradeep, and N. W. A. Lidula, "Modelling and simulation of a solar PV and battery based DC microgrid system," *International Conference on Electrical, Electronics, and Optimization Techniques, ICEEOT 2016*, no. i, pp. 1706–1711, 2016.

[15] S. M. Chen, T. J. Liang, and K. R. Hu, "Design, analysis, and implementation of solar power optimizer for DC distribution system," *IEEE Transactions on Power Electronics*, vol. 28, no. 4, pp. 1764–1772, 2013.

[16] D. Wang, F. Locment, and M. Sechilariu, "Modelling, simulation, and management strategy of an electric vehicle charging station based on a DC microgrid," *Applied Sciences (Switzerland)*, vol. 10, no. 6, 2020.

[17] F. Locment and M. Sechilariu, "Modeling and simulation of DC microgrids for electric vehicle charging stations," *Energies*, vol. 8, no. 5, pp. 4335–4356, 2015.

[18] A. Hamidi, L. Weber, and A. Nasiri, "EV charging station integrating renewable energy and second-life battery," *Proceedings of 2013 International Conference on Renewable Energy Research and Applications, ICRERA 2013*, no. October, pp. 1217–1221, 2013.

[19] Y. B. Aemro, P. Moura, and A. T. de Almeida, "Design and Modeling of a Standalone DC-Microgrid for Off-Grid Schools in Rural Areas of Developing Countries," *Energies*, vol. 13, no. 23, p. 6379, 2020.

[20] K. Kurohane, T. Senjyu, A. Yona, N. Urasaki, T. Goya, and T. Funabashi, "A hybrid smart AC/DC power system," *IEEE Transactions on Smart Grid*, vol. 1, no. 2, pp. 199–204, 2010.

[21] S. J. Ríos, D. J. Pagano, and K. E. Lucas, "Bidirectional Power Sharing for DC Microgrid Enabled by Dual Active Bridge DC-DC Converter," *Energies*, vol. 14, no. 2, p. 404, 2021.

[22] W. Panbao, W. Wei, X. Dianguo, and L. Ming, "An autonomous control scheme for DC micro-grid system," *IECON Proceedings (Industrial Electronics Conference)*, pp. 1519–1523, 2013.

[23] M. A. Jarrahi, F. Roozitalab, M. M. Arefi, M. S. Javadi, and J. P. S. Catalao, "DC microgrid energy management system containing photovoltaic sources considering supercapacitor and battery storages," *SEST 2020 - 3rd International Conference on Smart Energy Systems and Technologies*, 2020.

[24] L. Meng *et al.*, "Review on Control of DC Microgrids and Multiple Microgrid Clusters," *IEEE Journal of Emerging and Selected Topics in Power Electronics*, vol. 5, no. 3, pp. 928–948, 2017.

[25] Y. Han, X. Ning, P. Yang, and L. Xu, "Review of Power Sharing, Voltage Restoration and Stabilization Techniques in Hierarchical Controlled DC Microgrids," *IEEE Access*, vol. 7, pp. 149202–149223, 2019.

[26] M. H. Wang, S. C. Tan, C. K. Lee, and S. Y. Hui, "A configuration of storage system for DC microgrids," *IEEE Transactions on Power Electronics*, vol. 33, no. 5, pp. 3722–3733, 2018.

[27] Vítor Monteiro, João C. Ferreira, Andrés A. Nogueira Melendez, José A. Afonso, Carlos Couto, João L. Afonso, "Experimental Validation of a Bidirectional Three-Level dc-dc Converter for On-Board or Off-Board EV Battery Chargers", *IEEE IECON 2019 - Annual Conference of the IEEE Industrial Electronics Society*, Lisbon, Portugal, Oct. 2019, pp.3468-3473.

[28] Vítor Monteiro, Tiago J. C. Sousa, M. J. Sepúlveda, Carlos Couto, António Lima, João L. Afonso, "A Proposed Bidirectional Three-Level dc-dc Power Converter for Applications in Smart Grids: An Experimental Validation", *IEEE SEST 2019 - International Conference on Smart Energy Systems and Technologies*, Porto, Portugal, Sept. 2019, pp.1-6.